SoftwareX 33 (2026) 102480

Contents lists available at ScienceDirect

SoftwareX

journal homepage: www.elsevier.com/locate/softx

# Reducing complexity in photonic simulations: ZenScat — an efficient 2D RCWA solver

I. Lukosiunas [a,*], D. Gailevicius [a], K. Staliunas [a,b,c]

[a] Vilnius University, Faculty of Physics, Laser Research Center, Sauletekio Ave. 10, Vilnius, Lithuania
[b] ICREA, Passeig Lluis Companys 23, 08010, Barcelona, Spain
[c] UPC, Dep. de Fisica, Rambla Sant Nebridi 22, 08222, Terrassa (Barcelona), Spain

ARTICLE INFO

*Keywords:*
RCWA
FDTD
Scattering
GMR

ABSTRACT

We present a comprehensive solver implementation of a 2D Rigorous Coupled Wave Analysis (RCWA), tailored specifically for conformal thin multilayer devices and 2D photonic crystals with arbitrary interface profiles. Unlike traditional diffraction efficiency analysis, our approach emphasizes beam-shaping applications. Thus, our solver uniquely incorporates parameter sweeps across both wavelength and angular domains. This enables effective optimization of devices, such as low-pass spatial filters. Our software streamlines the design and analysis of complex photonic structures, broadening the practical application of RCWA methods and enabling the rapid development and optimization of novel photonic components.

## Metadata

See Table 1.

**Table 1**
Metadata.

| Nr | Code metadata description | Details |
|---|---|---|
| C1 | Current code version | *V1.1* |
| C2 | Permanent code link/repository of current version | https://github.com/ElectroMagneticAddict/ZenScat-UI. |
| C3 | Permanent link to reproducible capsule | *None* |
| C4 | Code versioning system used | *None* |
| C5 | Legal code licence | MIT |
| C6 | Software code languages, tools, and services used | Matlab |
| C7 | Compilation requirements, operating environments, and dependencies | '*MATLAB Coder*' for 'mex' files and '*MATLAB-Optimization Toolbox*' for optimization |
| C8 | Link to developer documentation/manual | https://github.com/ElectroMagneticAddict/ZenScat-UI/blob/main/APP_TUTORIAL.pdf. |
| C9 | Support email for questions | ignas.lukosiunas@ff.vu.lt |

## 1. Motivation and significance

Optical technology advancements are closely tied to devices featuring periodic geometry. Classical diffraction gratings are a well-known example [1,2]. Another important class includes devices utilizing Rayleigh-Wood anomalies [3,4], guided-mode resonances [5], bound states in the continuum [6], and similar phenomena [7]. Typically, these effects depend on periodic structures, which must precisely match preset conditions for periodicity, thickness, dielectric permittivity, and magnetic permeability [8]. Applications include biomedical uses [9], sensors [10], solar cell absorption enhancement [11,12], and security technologies [13]. A major advantage is their ease of fabrication and scalability.

* Corresponding author.
*Email address:* ignas.lukosiunas@ff.vu.lt (I. Lukosiunas).

https://doi.org/10.1016/j.softx.2025.102480
Received 30 July 2025; Received in revised form 19 November 2025; Accepted 3 December 2025
Available online 6 January 2026

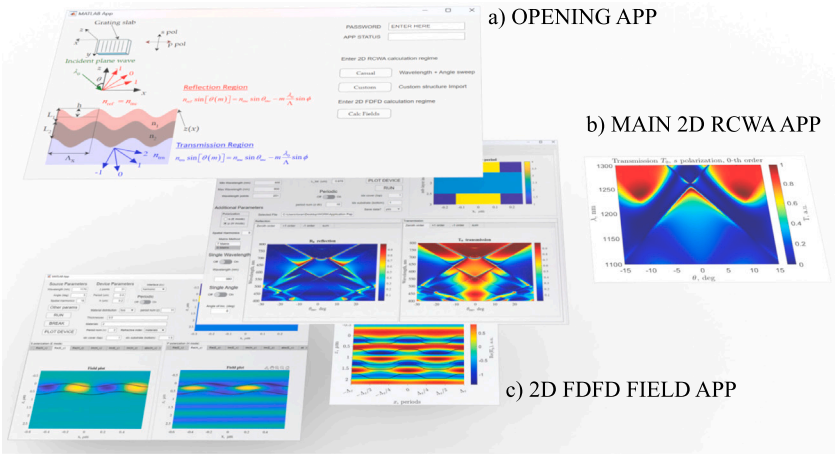


**Fig. 1.** 2D ZenScat application concept. The application opening app (a), which leads to 2D Casual and Import apps (b) and 2D FDFD field regime (c).

However, high-end applications require specialized expertise, forming a barrier to implementation [14]. Introducing novel methods, such as deep learning [15,16], further complicates this. Realistically, expertise in physics, numerical simulations, design algorithms, validation, and manufacturing processes is necessary, as each adds difficulty and hinders practical success.

Currently, brute-force numerical approaches are the main shortcut, employing methods such as finite difference time domain (FDTD) [17–20] or the faster yet more complex Finite Element Method. Although versatile, FDTD remains computationally demanding. Alternative methods like finite-difference frequency domain (FDFD) [21–23] or modal methods (e.g., rigorous coupled wave algorithm, RCWA [24]) reduce computational load but require advanced expertise in eigenvalue formalism [25]. Specialized methods, such as the Chandezon (C-method), are efficient but similarly complex [26–29].

We aim to lower these barriers by presenting our practical approach Fig. 1 for implementing the 2D RCWA method.

## 2. Software description

### 2.1. Code handling

The code is entirely written in the MATLAB environment, and its algorithm, dubbed as 'Playscript.m', is presented below.

The pseudo-algorithm is included in the supplementary material. The procedure, shown in Listing 1, begins by initializing the parameter `"struct"`, which contains the main geometry of the GMR filters and photonic crystals, as well as the source parameters, such as wavelength and angle of incidence. Then, these parameters are parsed into a `"grid" struct`, which saves/modifies those parameters for the `"device" struct`, mainly the distribution of permittivities of device layers. The `device struct` returns the permittivity convolution matrix and sub-layer thicknesses for the T matrix and S matrix layer connection procedures. That is how the main procedure is concluded and it is used in all parts of the software. The `"Playscript.m"` file contains those functions in the correct order for testing. We would like to add that the double-layer stacking can be achieved by setting `'distribution'` string to `'two'`, which is useful for constructing a periodic arrangement of a device in the z direction. In the current example, the distribution is set to `'all'`, where the refractive index and thickness layers are distributed arbitrarily. The current limitations of the algorithm are that the system of interest pertains to periodic boundary conditions in the $x$ coordinate (1D periodicity) and the negligence of the conical mount, so only TE and TM polarized plane wave source injection exist.

## 3. Illustrative examples

### 3.1. Comparison with FDTD variants

The first step in validating RCWA on complex periodic structures, such as harmonic gratings. Harmonic gratings, although they can be very efficiently simulated by the Chandezon method, pose an adequate validation challenge for the RCWA approach. They require a significant amount of subdivision. We examine a previous FDTD study of 1D sinusoidal profile nonpolarizing guided-mode-resonance (GMR) gratings with conformal dielectric thin films [30,31]. Normal incidence is analyzed, and the properties of single-mode and multimode nonpolarizing GMRs are explored. The study addresses the misalignment between the reflection responses of Transverse Electric (TE) and Transverse Magnetic (TM) polarizations. The same reflective properties can be maintained if a two-layered harmonic interface structure is implemented. An optimization approach is employed; it necessitates numerous iterations and, as previously discussed, is the most time-consuming aspect of the FDTD implementation.

One of the structures in question is shown in Fig. 2. The device parameters are as follows: upper layer thickness $L_1 = 182$ nm, lower layer thickness $L_2 = 120$ nm, lattice constant $\Lambda_x = 0.32$ μm, relief modulation depth $h = 154$ nm, substrate refractive index $n_{sub} = 1.516$. The layer material parameters are given by $n_1 = 1.781$ and $n_2 = 1.650$ for the upper and lower layers, respectively. Eleven spatial harmonics were used in the simulation and the simulation confirms peak diffraction efficiency in the reflection region at a wavelength of $\lambda_0 = 510.6$ nm.

This structure is a single-mode non-polarizing type-II GMR grating, and its spectral intensity dependence for the 0-th order is examined for both polarization cases, as a function of the incidence angle up to 5° (Fig. 2a and b). There is no deviation from the previously reported study. The normal-incidence dependence is shown in Fig. 2(c). The resonant wavelength is observed at 510.6 nm, closely matching the reported value of $\lambda = 511$ nm [30].

The second validation case involves biosensing, which can be achieved if any of the main parameters, materials, or geometries are sensitive to the environment. The classical rectangular-grating-on-substrate (Fig. 3a) in [31] is primarily used for the optical biosensing of the analytes. The idea presented is to create a monochromatic wavelength sensing device that does not require a spectrometer, as usual, but is so sensitive to ambient refractive index changes that a monochromatic detector is sufficient to register a resonance shift. Notably, a conical mount is considered; however, several results have been presented for 2D cases.

The grating results are simulated via FDTD using the (Ansys Lumerical Inc.) software and are presented in [31]. The grating parameters are: $n_{sup} = 1$, $n_{sub} = 1.47$, $h = 120$ nm, $L = 80$ nm, $\Lambda_x = 500$ nm,

```
%% Parameters
NH = 4;                % Spatial harmonic number
interface  = 'sin'; % Interface str - see 'Device'

% Additional interface params
interface_params = Int_Params;
%% ---------------------------------------------------------

% Layer stacking (thickness + refr idx)
% Params -> L1, L2, L3, n1, n2, n3
Params         = [0.182 0.120 1.781 1.650];
is_S_matrix  = 1;  % 0 if T matrix used

% Arbitrary distribution - 'all', periodic - 'two'
distribution = 'all';

if strcmp(distribution, 'all')
    % 1 refr index for 1 layer
    layer_num = ceil(length(Params)/2);
else
    % 2 refr indexes for all layers
    layer_num = length(Params) - 2;
    if layer_num == 0
        layer_num = 1;
    end
end
% Extract source and resolution parameters in [P]
[P] = Parameters(layer_num, distribution);
%% ---------- Regular RCWA algorithm ----------------------
for Mode = ['E', 'H'] % run for TE and TM pols
    % Assert main params
    P.Params = Params;
    % Build grid struct
    grid    = Grid(Params, interface, P);
    % Extract sub_L and ERC in device struct
    device = Device(NH, grid, ...
        interface, interface_params);
    %% ---------------------------------------------------------

    if is_S_matrix
        % compile to mex afterwards
        [TRN, REF] = Launch_RCWA_S(NH, grid, ...
        device, Mode, false);
    else
        % compile to mex afterwards
        [TRN, REF] = Launch_RCWA_T(NH, grid, ...
        device, Mode, false);
    end
    % Function for plotting diffraction efficiencies
    Plot_TRN_REF(TRN,REF,grid,Mode,Params,interface)
end
```

**Listing** 1: Main function handling of ZenScat. Parameters are chosen from [30].

$w_{gr} = 250$ nm. The offset of the resonance peaks in the wavelength spectrum for TE polarization is 2 nm, whereas for TM polarization it is 4 nm when compared with 2D RCWA results (see Fig. 3). We reason that the resonance shift results from the smaller mesh grid resolution used in the initial study to decrease the calculation time for the full 3D model.

In this section, we selected three studies that reported results obtained using FDTD, which we replicated here with our RCWA solver. Each study focused on different physical phenomena observed in resonant gratings. We show that the results are reproducible, but in some cases they involve hidden parameters that are not well declared and may distort spectral features at shorter wavelengths.

### 3.2. Comparison with other 2D RCWA variants

After validating the selected results derived through FDTD simulations, we also provide an analysis featuring two RCWA studies.

The first concerns predicting how the spectral sensitivity of the transmission and reflection properties, as a function of incident angle, can be employed in spatial filtering [32]. The concept, introduced by the authors, is that losses of the high-spatial-frequency components occur via diffraction, whereas the cleaned beam is reflected. A single thin layer with a simple rectangular surface-relief grating can exhibit narrow-angle reflection. It is also notable because it is essentially lossless; its design does not require absorbing materials. Elsewhere, the concept has been proven helpful in feedback tailoring, as seen in laser outcoupling mirrors [33].

To keep the approach simple, we have calculated and validated the results reported in [32], as shown in Fig. 4. The angular width of the TE reflection spectrum is 0.1°, which corresponds to 1.7 mrad. Filtering is achieved by diffraction (represented by the red solid and dashed lines) and zeroth-order transmittance (illustrated in orange). The simulations for this work were performed using the "ZenScat" interface. The parameters of the GMR device used are as follows: $n_g = 2.52$ for the $TiO_2$ film, $n_{sub} = 1.54$, $n_{sup} = 1$, grating period $\Lambda_x = 696$ nm, film thickness $L = 578$ nm, and grating amplitude $h = 210$ nm.

### 3.3. DFB specifics

In this section, we present a study on the convergence of materials with absorption losses, as well as those with gain, in distributed-feedback (DFB) systems. Passive and lossy DFB systems are well known [34]. Gain systems [35–38] are relatively recent and feature the same challenges as lossy systems. We also extend their parameter optimization using the third ZenScat application (see the digital supplement), where the genetic algorithm is implemented via MATLAB's external library. The primary strength of genetic optimization lies in the use of parallel pooling, which enables the rapid identification of the best available extrema in phase space. The goal of such an application is to maximize or minimize diffraction efficiency values (as well as absorption or gain) in distributed systems.

The optimization is performed via the `device's import` function (see digital supplementary information for the DFB Python main files). The parameters are summarized in the Table 2 and the device concept is shown in Fig. 5(a).

The results are summarised in Fig. 5. The enhancement of gain and absorption at normal incidence is achieved in DFB systems. The genetic algorithm is capable of quickly finding local extrema and yielding enhanced values of absorption and gain via GMR. We note that such optimization problems can be used to minimize or maximize diffraction efficiencies in the reflection and transmission regimes. We illustrate three cases of media with an imaginary refractive index. The first calculated case, shown in Fig. 5(b), features a perovskite gain material in the last layer. The periodicity corresponds to a sub-wavelength operating regime for the device. Enhanced gain is obtained at normal incidence during the optimization procedure. The first near-normal-incidence resonances yield amplification of up to 20 dB; however, second-order resonances at larger angles of oblique incidence (5–10°) operate near the sub-wavelength regime, close to Wood's anomalies[39], which, when crossed, mark the onset of this regime. The metal absorber case, shown in Fig. 5(c), provides full reflectance except at the resonant points of enhanced coupling between the incident beam and the absorptive layer. In this regime, angle-dependent light absorption is achieved. The optimization is also performed at normal incidence. The large imaginary part of the refractive index leads to nearly full reflection, except at the absorption points. Silver was used for this case. However, in the weak-absorber case (silicon, whose diffraction efficiencies and absorption are illustrated in Fig. 5d), a single-layer structure exhibits narrow-band absorption, resulting from GMR coupling with the absorptive layer.

### 3.4. T matrix and S matrix performance

While the results above are valid and reproducible, the question of how to quantify performance remains. This refers to the computational

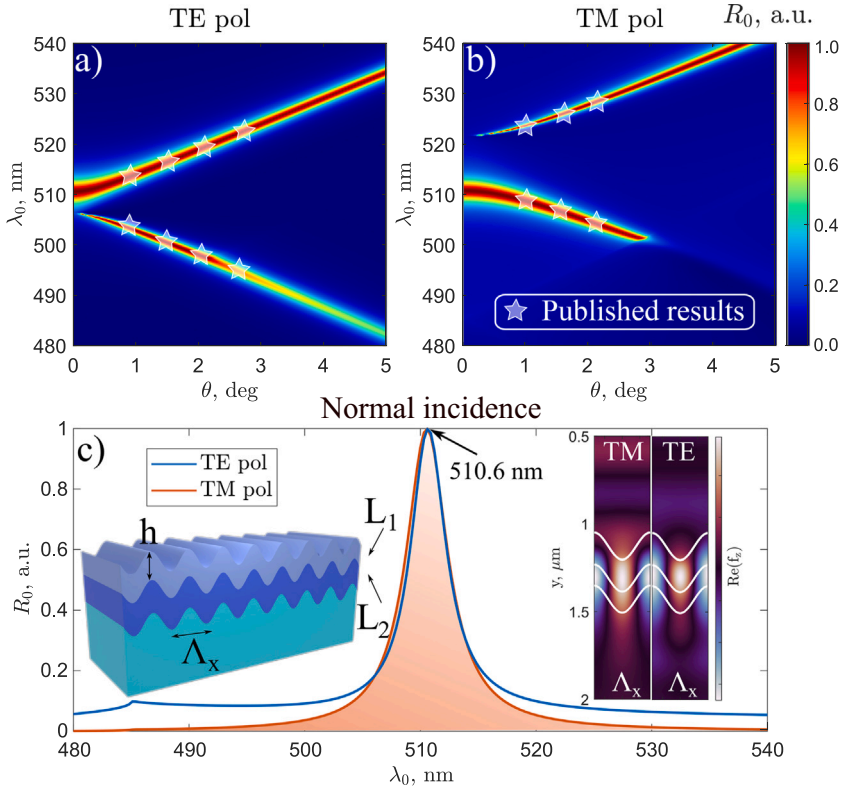


**Fig. 2.** RCWA derived reflection spectra distributions of TE polarization (a), TM polarization (b), and their intersection at normal incidence with their respective fields (stars show data from [30] (c) for double-layered harmonic gratings first reported in [30].

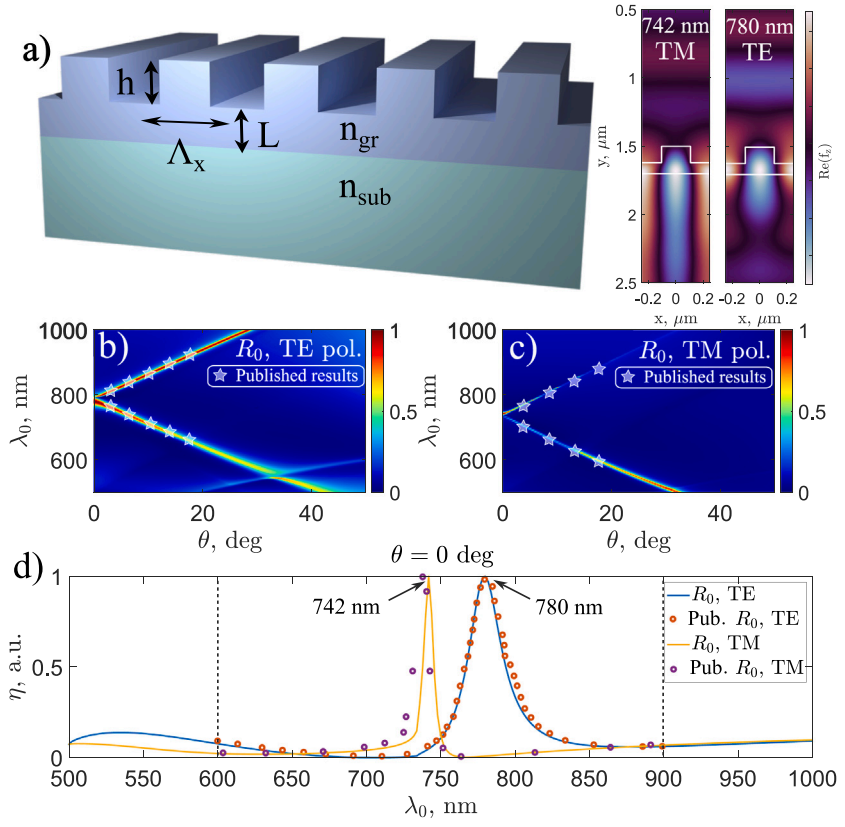


**Fig. 3.** Guided mode resonance reflection spectra of $SiN_4$ grating via the RCWA approach. Accordingly, (a) for TE (b) and TM (c) polarizations, as well as diffraction efficiencies for both polarizations at normal incidence (d). The structure is derived from [31] and star symbols show datapoints from the initial study.

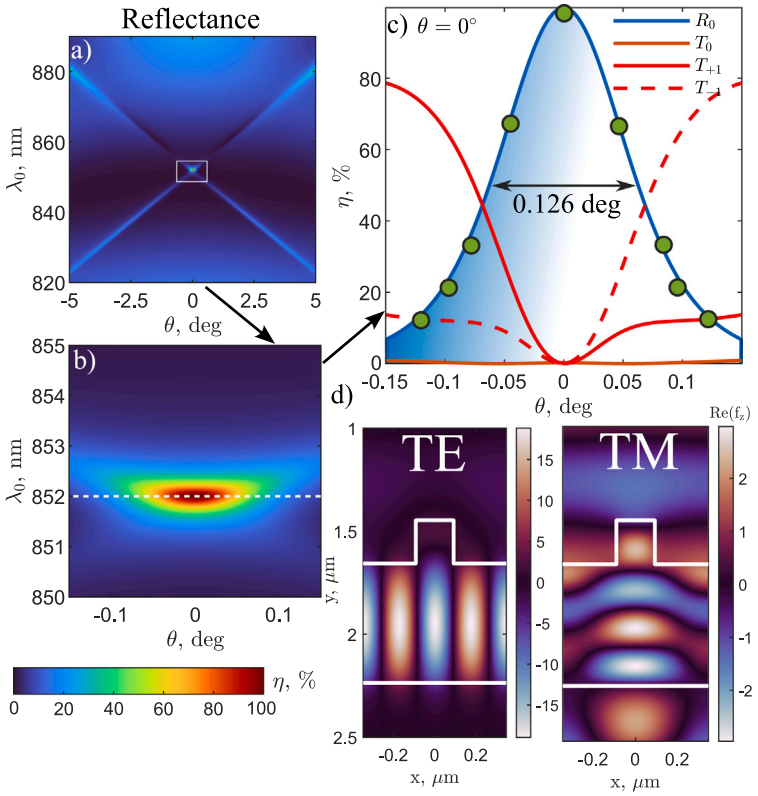


**Fig. 4.** Magnusson's spatial filtering concept [32] here simulated in full with "ZenScat". The zeroth order reflection is denoted at a) zoomed at b), the diffraction efficiency is present at (green dots are datapoints from [32]) c) for the thin film GMR sup-wavelength grating, shown at d). (For interpretation of the references to colour in this figure legend, the reader is referred to the web version of this article).

**Table 2**
DFB parameters achieved through genetic optimization, given $n_{sub} = 1.5$.

| $\Lambda_x$, μm | $L_1$, μm | $L_2$, μm | $L_3$, μm | $n_{gr}$ | $n_c$ |
|---|---|---|---|---|---|
| 0.4027 | 0.1578 | 0.01767 | 0.8117 | 1.5 | $2.04 + 10^{-3}j$ |
| 0.5336 | 0.1098 | 0.1006 | 0.1 | 2.0 | $0.04 - 4.80j$ |
| 0.343 | 0.1606 | 0.1858 | 0.2845 | 2.0 | $3.4 - 10^{-3}j$ |

complexity problem. The other critical question here is which particular sub-algorithm to choose in order to minimize numerical error and maximize computational throughput.

Compared to the Scattering Matrix Method, the Enhanced Transmittance Matrix (ETM) approach can improve the computational efficiency of the RCWA algorithm. However, its accuracy needs to be evaluated for GMR filters and photonic crystals. As a specific example, we chose the sinusoidal holographic layer-type structure [40–43]. The selectivity of such structures for polarization states is well known [44] and can be used as a benchmark. The Fig. 6 summarises the relevant results.

The ETM approach is abbreviated as the T-matrix method [45], whereas the scattering matrix method is abbreviated as the S-matrix method [46]. The device is constructed within the preparatory part of the implementation before launching 2D RCWA calculations for a wavelength sweep at normal incidence (dispersionless case). For a single wavelength ($\lambda = 1$ $\mu$m), the results are presented in Fig. 6(a) and (b). The compiled version provides an approximately twofold speed improvement using the MATLAB Coder app. An unusual feature is observed in Fig. 6(b), where the computation time is much longer for spatial harmonic counts lower than 11. The compiled version allows us to overcome this behavior for both the S- and T-matrix methods. The results presented in Fig. 6(c) and (d) assess the relative accuracy for the same structure. These quantities are computed as $\Delta\eta_T = |T_0^{(\text{Tmatrix})} - T_0^{(\text{Smatrix})}|$ and $\Delta\eta_R = |R_0^{(\text{Tmatrix})} - R_0^{(\text{Smatrix})}|$. The mismatch values are on the order of approximately $-14$, which is a very small value concerning real physical systems.

Furthermore, we checked the convergence of the simplest rectangular devices, which are the spatial filter as shown in Fig. 4 and the optimized DFB structure as shown in Fig. 5(c) - metallic absorber. The convergence graphs of such structures are shown for their specific wavelengths at normal incidence (see Fig. 6e and f). The wavelengths of interest are $\lambda_0 = \{852, 700\}$ nm, respectively, for which such devices operate in the non-sub-wavelength regime. This is due to the $\lambda_0 < \Lambda_x n_{\text{sub}} = \{1044, 800\}$ at normal incidence for the rectangular filter and the metallic DFB absorber, respectively. Such structures pertain to $\pm 1$ diffraction orders in such a regime. We identified 6 spatial harmonics, which give $N = 13$ total spatial harmonics in the numerical model.

The calculation speed was compared with the modal method used in the "MC Grating" software [47]. The results are summarized in Table 3.

The computation was performed on a relatively older hardware setup, an Intel (R) Core (TM) i5-33320 M CPU at 2.6 GHz, to facilitate this comparison. The calculation was performed for a parameter sweep of a trapezium-shaped interface with the following parameters: $N_z = 11$, $N_x = 1028$, $N_h = 11$, $n_\lambda = 101$, $n_\theta = 101$, where these correspond to the numbers of discrete layers along the $z$ and $x$ directions, the number of spatial harmonics, the number of wavelength samples, and the number of angles of incidence, respectively. Note that these results are obtained only when using compiled C++ MEX files (denoted as `mex`) in MATLAB (version 2023 b, MathWorks, Inc.) generated with the MATLAB Compiler™. Reflection and transmission calculations were performed for the T-matrix method separately, thereby reducing the number of matrix operations in the function and achieving computational speeds that

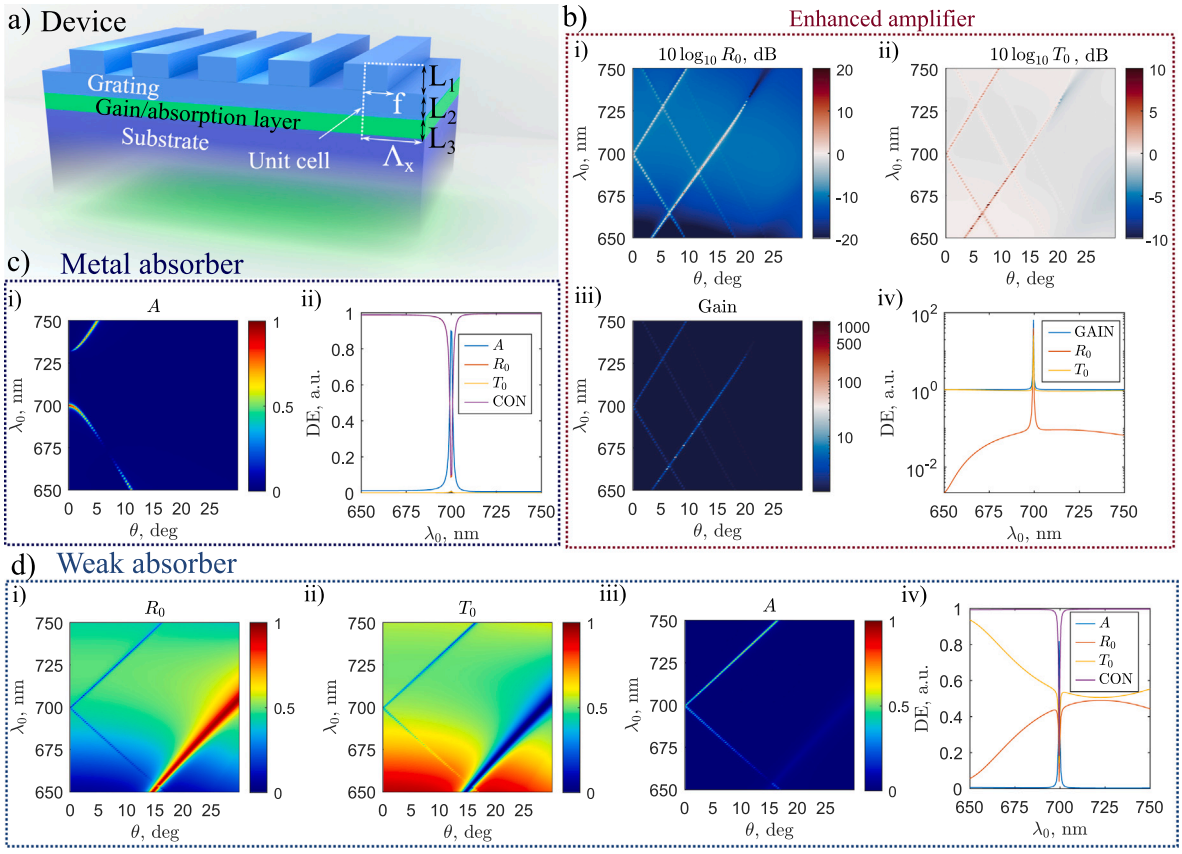


**Fig. 5.** DFB system which utilizes GMR-based coupling from the grating with gain/absorption layer (a). The enhanced gain spectrum is shown in b), given the Diffraction Efficiencies (DE) $R_0$ and $T_0$, as well as values for normal incidence (shown in b, iv). The absorption $A$ profiles of the metallic absorber are shown in c). The weak absorber's DE characteristics are provided in d).

**Table 3**
Computation speed comparison (in time). Structure provided in Supplementary Material.

| Polarization state | RCWA (S Matrix), s | RCWA (T matrix), s | MC Grating Ver. 2022–12-08 (FMM), s |
|---|---|---|---|
| TE (s pol) | 34.77 | 20.48 | ≈ 50 |
| TM (p pol) | 39.15 | 27.46 | ≈ 60 |

are approximately twice as fast as those of the commercial software. If the T-matrix or S-matrix functions are not compiled, they are approximately twice as slow, so the T-matrix method's computational speed becomes comparable to that of the commercial Fourier Modal Method (FMM) described in [47].

## 4. Impact

We acknowledge previous specialized attempts, including model enhancements for simplicity and performance [48–50]. However, we observe a significant lack of validation studies demonstrating the reliability of RCWA approaches for a diverse range of applications. This justifies a transition from costly but straightforward methods to rapid, however, beginner-averse methods. To achieve this, we provide our implementation as the solver interface described in the Supplementary Material and the compiled solver in the Digital Supplement of the external repository, along with the accompanying raw data (see [51]). We explain the various aspects of the preferred method for our chosen numerical approach and provide examples of the new information that can be extracted from these structures, along with a comparison of the achievable performance. Hence, we offer contributions to the field of computational photonics with the 'ZenScat User Interface':

- **Computationally faster 2D RCWA compared to commercial software** in a MATLAB environment. The application is designed for sharing with the academic community, which is twice as fast as the most appropriate alternative to the MC grating's [47] FMM solver.
- **Qualitative comparison of computational speed** between Transmittance and Scattering matrix methods, compiled and pure MATLAB codes in the MATLAB environment. We also compare zeroth-order diffraction efficiencies calculated with both methods.
- **Cross-validation** of published results encompasses Guided Mode Resonance filters and a dispersive coupler. This is done for results calculated with commercial FDTD environments and other RCWA implementations, which are widely presented in the literature.
- **Contribution to reproducibility in science**; as reproducibility studies are rare and sometimes passively discouraged, it can eventually result in a lack of disclosure or misleading disclosure [52,53]. We achieve a secondary objective of making our ethical contribution in computational studies [54]. We also expand the data that is not proposed
- **Genetic Optimization** applied for arbitrary interface profiles and their topology.
- **The User Interface** for reducing the barrier to entry for using 2D RCWA as a genetic algorithm.

Supplementary Information contains instructions on reproducing all results for added transparency and applicability, as provided using "ZenScat".

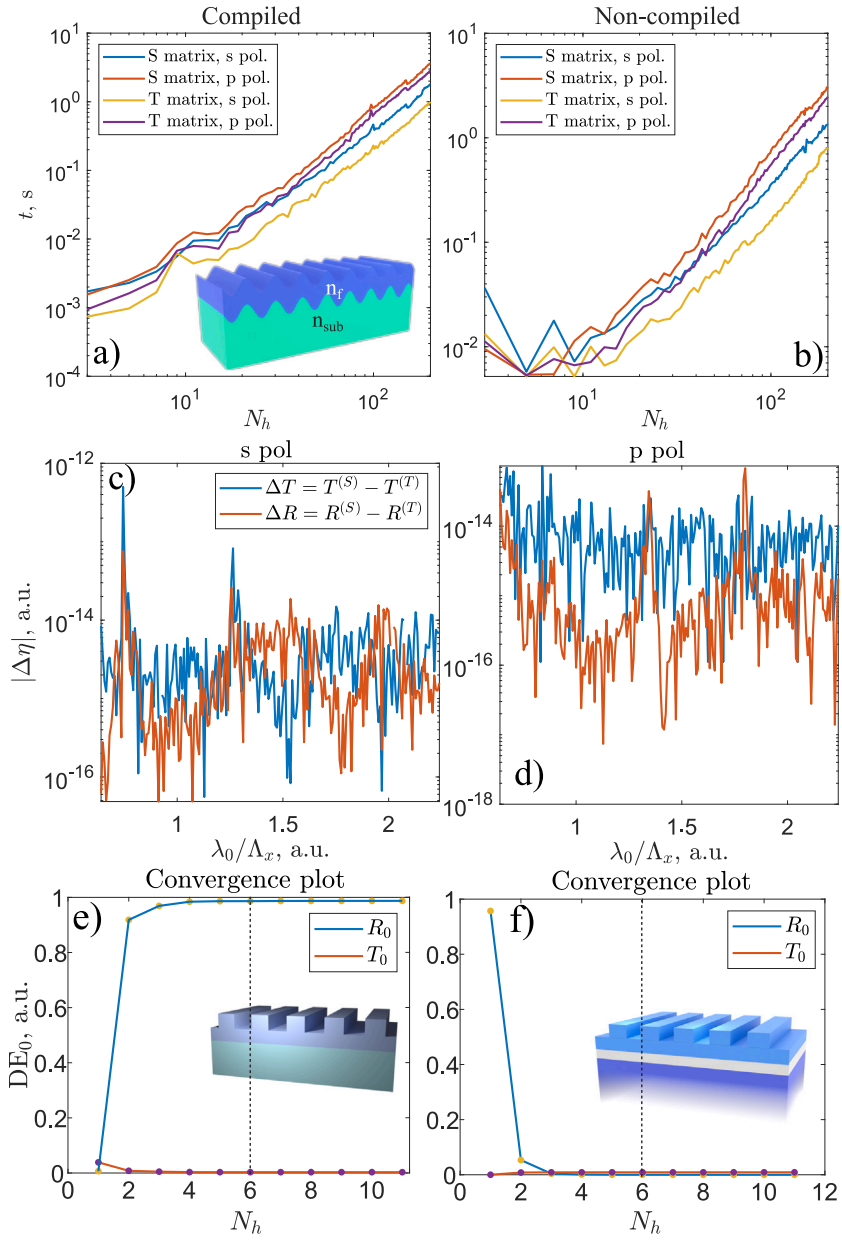


**Fig. 6.** Algorithm performance with compiled (a) and non-compiled (b) matrix methods. The diffraction efficiency errors for monolayered GMR filter for s and p polarizations (c,d) for $\theta = 15°$ of incidence. The convergence plots for the spatial filter of Fig. 4 and the metallic DFB of Fig. 5 c) are presented in e) and f), respectively.

## 5. Conclusions

To reiterate, applied computational physics currently faces issues in choosing FDTD methods over more suitable numerical alternatives. Many problems involving periodic or finely modulated relief structures can be efficiently solved using methods like RCWA. Despite this, RCWA is frequently overlooked due to the advanced intuition required for implementation. However, RCWA significantly reduces the requirements for discretization and computational load. We address this issue by developing and validating our solver, "ZenScat," across several intriguing structures.

Dielectric resonant gratings, due to their non-lossy characteristics, are particularly noteworthy. We identified three cases where RCWA would have been advantageous and conducted validation studies to support this finding. Our results successfully reproduced major findings but revealed challenges, such as hidden parameters and qualitative divergence related to mesh resolution—common issues in FDTD studies but well-handled by landmark RCWA cases. Additionally, we examined lossy and gain structures to further demonstrate method validity, where convergence can be a challenge.

From a technical viewpoint, we analyzed the performance of the S- and T-matrix methods, finding a slight advantage for the T-matrix method. Moreover, comparing the matrix methods with an alternative FMM implementation showed approximately a two-fold improvement in calculation speed.

In summary, our "ZenScat" solver provides a valuable tool for computational photonics, validated against multiple previous studies. We expect it to significantly accelerate numerical tasks in advanced sensor and device research, facilitating rapid validation for various resonant photonic devices.

## CRediT authorship contribution statement

**I. Lukosiunas:** Writing – original draft, Visualization, Validation, Software. **D. Gailevicius:** Writing – original draft, Resources, Conceptualization. **K. Staliunas:** Supervision.

## Declaration of competing interest

The authors declare the following financial interests/personal relationships which may be considered as potential competing interests:

Ignas Lukosiunas reports that financial support was provided by the Vilnius University Faculty of Physics. If there are other authors, they declare that they have no known competing financial interests or personal relationships that could have appeared to influence the work reported in this paper.

## Acknowledgements

Author I.G. acknowledges funding from the "Universities' Excellence Initiative" program by the Ministry of Education, Science and Sports of the Republic of Lithuania under the agreement with the Research Council of Lithuania (project No. S-A-UEI-23–6). D.G. acknowledges support by the Research Council of Lithuania (project No. S-MIP-23–49).

## Appendix A. Supplementary data

Supplementary data to this article can be found online at doi: 10.1016/j.softx.2025.102480.

## References

[1] Sahoo P, Coates E, Silver C, Li K, Krauss TF. On the reproducibility of electron-beam lithographic fabrication of photonic nanostructures. Sci Rep Apr 2024;14. https://doi.org/10.1038/s41598-024-58842-w
[2] Plukys M, Grineviciute L, Nikitina J, Gailevicius D, Staliunas K. Enhancement of brightness in microchip laser with angular filtering mirrors. Opt Laser Technol 2025;181:111904. https://doi.org/10.1016/j.optlastec.2024.111904. https://www.sciencedirect.com/science/article/pii/S0030399224013628.
[3] Amin M, Yoon JW, Magnusson R. Optical transmission filters with coexisting guided-mode resonance and Rayleigh anomaly. Appl Phys Lett 2013;103:131106. https://doi.org/10.1063/1.4823532
[4] Lukosiunas I, Grineviciute L, Nikitina J, Gailevicius D, Staliunas K. Extremely narrow sharply peaked resonances at the edge of the continuum. Phys Rev A 2023;107:L061501. https://doi.org/10.1103/PhysRevA.107.L061501.
[5] Huo P, Chen W, Zhang Z, Zhang Y, Liu M, Lin P, Zhang H, Chen Z, Lezec H, Zhu W, Agrawal A, Peng C, Lu Y, Xu T. Observation of spatiotemporal optical vortices enabled by symmetry-breaking slanted nanograting. Nature Communications Apr 2024;15. https://doi.org/10.1038/s41467-024-47475-2
[6] Hsu CW, Zhen B, Stone AD, Joannopoulos J, Soljačić M. Bound states in the continuum. Nat Rev Mater 2016;1:16048. https://doi.org/10.1038/natrevmats.2016.48
[7] Wang PY, Herrero R, Botey M, Cheng YC, Staliunas K. Translationally invariant metamirrors for spatial filtering of light beams. Phys Rev A 2020;102:013517. https://doi.org/10.1103/PhysRevA.102.013517.
[8] Babayigit C, Grinevičiutė L, Nikitina J, Melnikas S, Gailevicius D, Staliunas K. Inverse designed photonic crystals for spatial filtering. Appl Phys Lett Jun 2023;122. https://doi.org/10.1063/5.0150756
[9] Deb H, Srisuai N, Boonruang S, Jolivot R, Promptmas C, Mohammed W. 3d-printed guided mode resonance readout system for biomedical and environmental applications. Eng J 2021;25:35–43. https://doi.org/10.4186/ej.2021.25.6.35
[10] Keshmiri H, Armin F, Elsayad K, Schreiber F, Moreno-Sereno M. Leaky and waveguide modes in biperiodic holograms. Scientific Rep 2021;11:10991. https://doi.org/10.1038/s41598-021-89971-1
[11] Peng W, Zhang G, Lv YY, Qin L, Qi K. Ultra-narrowband absorption filter based on a multilayer waveguide structure. Opt Express 2021;29(10):14582–600. https://doi.org/10.1364/OE.421206. https://opg.optica.org/oe/abstract.cfm?URI=oe-29-10-14582.
[12] Lee Y-C, Huang C-F, Chang J-Y, Wu M-L. Enhanced light trapping based on guided mode resonance effect for thin-film silicon solar cells with two filling-factor gratings. Opt Express 2008;16:7969–75. https://doi.org/10.1364/OE.16.007969
[13] Quaranta G, Basset G, Martin O, Gallinet B. Recent advances in resonant waveguide gratings. Laser Photonics Rev Jul 2018;12. https://doi.org/10.1002/lpor.201800017
[14] Lee Y-C, Ho Y-L, Lin B-W, Chen M-H, Xing D, Daiguji H, Delaunay J-J. High-q lasing via all-dielectric bloch-surface-wave platform. Nature Communications Oct 2023;14. https://doi.org/10.1038/s41467-023-41471-8
[15] Clini de Souza A, Lanteri S, Hernández-Figueroa HE, Abbarchi M, Grosso D, Kerzabi B, Elsawy M. Back-propagation optimization and multi-valued artificial neural networks for highly vivid structural color filter metasurfaces. Scientific Rep 2023;13(1):21352. https://doi.org/10.1038/s41598-023-48064-x. arXiv:2310.01234.
[16] Cao X, Lian Y, Li J, Wang K, Ma C. Unsupervised multi-level spatio-spectral fusion transformer for hyperspectral image super-resolution. Opt Laser Technol April 2024;176:111032. https://doi.org/10.1016/j.optlastec.2024.111032. https://linkinghub.elsevier.com/retrieve/pii/S0030399224004900.
[17] Choi M, Park J, Shin J, Keawmuang H, Kim H, Yun J, Seong J, Rho J. Realization of high-performance optical metasurfaces over a large area: a review from a design perspective. npj Nanophotonics 2024;1(1):31, published on 2024/08/30. https://doi.org/10.1038/s44310-024-00029-2.
[18] Wei Y, Yang Y, Zhao Q, Ma Y, Qiang M, Fu L, Liu Y, Zhang J, Qu Z, Que W. Numerical simulation technologies in solar-driven interfacial evaporation processes. Small 2024;20(32):2312241. https://doi.org/10.1002/smll.202312241. https://onlinelibrary.wiley.com/doi/pdf/10.1002/smll.202312241.
[19] Yee K. Numerical solution of initial boundary value problems involving maxwell's equations in isotropic media. IEEE Trans Antennas Propag 1966;14(3):302–7. https://doi.org/10.1109/TAP.1966.1138693
[20] Taflove A, Hagness SC. Computational electrodynamics: the finite-difference time-domain method. 3rd ed. Norwood; 2005.
[21] Shin W, Fan S. Choice of the perfectly matched layer boundary condition for frequency-domain maxwell's equations solvers. J Comput Phys 2012;231(8):3406–31. https://doi.org/10.1016/j.jcp.2012.01.013. https://www.sciencedirect.com/science/article/pii/S0021999112000344.
[22] Rumpf RC. electromagnetic and photonic simulation for the beginner: finite difference frequency-domain in MATLAB. Artech House; 2022.
[23] Rumpf RC, Garcia CR, Berry EA, Barton JH. Finite-difference frequency-domain algorithm for modeling electromagnetic scattering from general anisotropic objects. Progress In Electromagnetics Research B 2014;61:55–67. https://doi.org/10.2528/PIERB14071606
[24] Edmunds J. Python implementation of rigorous coupled wave analysis. 2022, https://pypi.org/project/rcwa/ [accessed: 2022-Oct-1].
[25] Jang HT, Yi JC. Comparison of rigorous coupled-wave analysis and finite difference time domain method on dielectric gratings. In: 2021 IEEE region 10 symposium (TENSYMP); 2021. p. 1–4. https://doi.org/10.1109/TENSYMP52854.2021.9550974
[26] Chandezon J, Raoult G, Maystre D. A new theoretical method for diffraction gratings and its numerical application. Journal of Optics 1980;11(4):235–41. https://doi.org/10.1088/0150-536x/11/4/005.
[27] van der Aa NP. Diffraction grating theory with rcwa or the c method. In: Di Bucchianico A, Mattheij RMM, Peletier MA, editors. Progress in industrial Mathematics at ECMI 2004. Berlin, Heidelberg: Springer Berlin Heidelberg; 2006. p. 99–103.
[28] Chen S, Deng H. Efficient simulation of the reflectance/transmittance for diffracting structures with small incident angle in the incident plane parallel to grating lines. Optik Int J Light Electron Opt 2013;124(17):3072–8. https://doi.org/10.1016/j.ijleo.2012.09.028. https://www.sciencedirect.com/science/article/pii/S0030402612007632.
[29] Kang C, Park C, Lee M, Kang J, Jang MS, Chung H. Large-scale photonic inverse design: computational challenges and breakthroughs. Nanophotonics 2024;13(20):3765–92 [cited 2024-09-10]. doi:https://doi.org/10.1515/nanoph-2024-0127.
[30] Li YY, Hu C, Wu YC, Chen JJ, Feng HH. Numerical investigation of one-dimensional nonpolarizing guided-mode resonance gratings with conformal dielectric films. Opt Express 2013;21(1):345–57. https://doi.org/10.1364/OE.21.000345. https://opg.optica.org/oe/abstract.cfm?URI=oe-21-1-345.
[31] Sarkar S, Devinder S, Sahoo PK, Joseph J. Exploring tunable single-wavelength detection schemes for guided-mode resonance sensors. Optics & Laser Technology 2024;177:111107. https://doi.org/10.1016/j.optlastec.2024.111107. https://www.sciencedirect.com/science/article/pii/S0030399224005656.
[32] Niraula M, Yoon JW, Magnusson R. Concurrent spatial and spectral filtering by resonant nanogratings. Opt Express 2015;23(18):23428–35. https://doi.org/10.1364/OE.23.023428.
[33] Aubourg A, Rumpel M, Didierjean J, Aubry N, Graf T, Balembois F, Georges P, Ahmed MA. 1617 NM emission control of an ER:YAG laser by a corrugated single-layer resonant grating mirror. Opt Lett 2014;39(3):466. https://doi.org/10.1364/ol.39.000466
[34] Bertolotti M. Waves and fields in optoelectronics. Opt Acta Int J Opt 1985;32(7):748. https://doi.org/10.1080/716099690
[35] Sun S, Xiao S, Song Q. Distributed feedback laser based on single crystal perovskite. In: Journal of Physics: conference series, vol. 844. IOP Publishing; 2017, p. 012022.
[36] Bonal V, Quintana JA, Villalvilla JM, Boj PG, Díaz-García MA. Controlling the emission properties of solution-processed organic distributed feedback lasers through resonator design. Scientific Reports 2019;9(1):11159.
[37] Tian X, Wang R, Xu Y, Lin Q, Cao Q. Triangular micro-grating via femtosecond laser direct writing toward high-performance polarization-sensitive perovskite photodetectors. Adv Optical Mater 2022;10(19):2200856.
[38] Allegro I, Bonal V, Mamleyev ER, Villalvilla JM, Quintana JA, Jin Q, Díaz-García MA, Lemmer U. Distributed feedback lasers by thermal nanoimprint of perovskites using gelatin gratings. ACS Appl Mater Interfaces 2023;15(6):8436–45.
[39] Sarrazin M, Vigneron J-P, Vigoureux J-M. Role of wood anomalies in optical properties of thin metallic films with a bidimensional array of subwavelength holes. Physical Review B 2003;67(8):085415.
[40] Neviere M, Petit R, Cadilhac M. About the theory of optical grating coupler-waveguide systems. Opt Commun 1973;8(2):113–7. https://doi.org/10.1016/0030-4018(73)90150-8.

[41] Neviere M, Vincent P, Petit R, Cadilhac M. Systematic study of resonances of holographic thin film couplers. Opt Commun 1973;9(1):48–53. https://doi.org/10.1016/0030-4018(73)90333-7.
[42] Neviere M, Vincent P, Petit R, Cadilhac M. Determination of the coupling coefficient of a holographic thin film coupler. Opt Commun 1973;9(3):240–5. https://doi.org/10.1016/0030-4018(73)90296-4.
[43] Jacques A, Ostrowsky DB. The grating coupler: comparison of theoretical and experimental results. Opt Commun 1975;13(1):74–7. https://doi.org/10.1016/0030-4018(75)90161-3.
[44] Quaranta G, Basset G, Martin OJF, Gallinet B. Recent advances in resonant waveguide gratings. Laser Photonics Rev Sep 2018;12(9). https://doi.org/10.1002/lpor.201800017.
[45] Moharam MG, Pommet DA, Grann EB, Gaylord TK. Stable implementation of the rigorous coupled-wave analysis for surface-relief gratings: enhanced transmittance matrix approach. J Opt Soc Am A 1995;12(5):1077–86. https://doi.org/10.1364/JOSAA.12.001077.
[46] Rumpf R. Improved formulation of scattering matrices for semi-analytical methods that is consistent with convention. Prog In Electromagn Res B 2011;35:241–61. https://doi.org/10.2528/PIERB11083107
[47] Lyndin BUN. Modal and c methods grating design and analysis software. 1999, https://mcgrating.com/ [accessed: 2022-Oct-30].
[48] Liu V, Fan S. S4: a free electromagnetic solver for layered periodic structures. Comput Phys Commun 2012;183(10):2233–44. https://doi.org/10.1016/j.cpc.2012.04.026. https://www.sciencedirect.com/science/article/pii/S0010465512001658.
[49] Kim C, Lee B. Torcwa: Gpu-accelerated Fourier modal method and gradient-based optimization for metasurface design. Comput Phys Commun 2023;282:108552. https://doi.org/10.1016/j.cpc.2022.108552. https://www.sciencedirect.com/science/article/pii/S0010465522002715.
[50] Lou B, Fan S. RCWA4D: electromagnetic solver for layered structures with incommensurate periodicities. Comput Phys Commun 2025;306:109356. https://doi.org/10.1016/j.cpc.2024.109356. https://www.sciencedirect.com/science/article/pii/S0010465524002790.
[51] Ignas Lukosiunas. Zenscat-UI. 2025, https://github.com/ElectroMagneticAddict/ZenScat-UI [Accessed: 2025-Jun-25].
[52] Aboites V, Barmenkov Y. Scientific replicability: two cases of study in laser Physics. Open J Philos 2022;12(4):510–22. https://doi.org/10.4236/ojpp.2022.124034.
[53] Tang BL. Publishing important work that lacks validity or reproducibility–pushing frontiers or corrupting science? Accountability in Research 2024:1–21.
[54] Hermann S, Fehr J. Documenting research in simulation science to enhance understanding for reusability. Royal Soc Open Sci Oct 2024;11(10). https://doi.org/10.1098/rsos.240776. https://royalsocietypublishing.org/doi/10.1098/rsos.240776.